2018 European Control Conference (ECC)
June 12-15, 2018. Limassol, Cyprus

Online power meter calibration for accurate cyclist power control

Dario Nava, Simone Formentin, Sergio M. Savaresi

Abstract— **This paper deals with cyclist power estimation in bicycles via a power meter device measuring the torque applied to the pedal. In order to guarantee the correctness of power estimation, it can be shown that the angular displacement between the crank arm longitudinal axis and the torque measurement axis must be accurately known. In this work, an online algorithm is developed to estimate such an angle, which can also vary along the time due to mechanical stress, without the need of a periodic calibration procedure. All these features make the resulting power estimation suitable for real-time cyclist power control. Experimental results show the effectiveness of the proposed estimation procedure on real road tests.**

I. INTRODUCTION

In professional cycling, the knowledge of critical quantities like output power or cadence can help to improve the performances of an athlete. In particular, the output power, related to the energy consumed by the cyclist, is considered to be the most important variable for optimizing the overall efficiency [1], thus making power meters the most critical technology from this point of view.

Such sensors can be classified in different categories, depending on the measurement strategy [2]. A direct approach to measure the cyclist power output is to measure the forces applied to the pedals using, e.g., a force sensor mounted on the bottom surface of the cycling shoe [7]. However, this approach is generally costly and will not be considered here.

A more common approach is based on the measurement of the torque transmitted by the cyclist to the bicycle drive-train system. The basic idea is to use strain gauges to convert the microscopic deformation of specific mechanical parts of the drive-train into a torque value. Such deformations can be measured in different positions, e.g.:

- at the crank set, with strain gauges mounted on the spider or on the crank arms. In this configuration the power meter substitutes interely the crank set. The most used devices of this kind, which is usually taken as a reference for output power measure in bicycles, are the SRM® power meters [3]. The accuracy of the SRM® devices has been assessed in [4],[5];
- at the crank arms, as explained in [6], with a power meter that substitutes only one or both the crank arms. Since these kind of sensor are very easy to fix to the bicycle frame, many commercial solutions are available, like Stages Cycling© and 4iiii® power meters;
- at the rear hub of the bicycle, measuring the torque trasmitted by the chain to the rear wheel (PowerTap© Hub [4]);
- at the axles of one or both pedals. As for crank arm solutions, these power meters are easy to install and can be mounted on different bicycles. However, they need a calibration procedure in order to estimate the installation angle, which cannot be known, as the devices are manually fixed to the crank arm by the user. An example is Garmin® Vector™.

In this paper, the latter case, namely a power meter sensor which measures the torque applied at the axle of the left pedal, is considered and analyzed in detail. Such a power meter has to be mounted on the left crank arm of the bicycle and connects the pedal to the crank arm itself. In order to correctly compute the output power, a suitable estimation of the angular displacement between the crank arm longitudinal axis and the torque measurements axis is needed, not to lead to inaccurate power estimates.

Here, an online estimation algorithm for such an angle is proposed. The strategy relies only on the inertial measurements coming from the Inertial Measurement Unit (IMU) embedded into the power meter device. With the proposed strategy, not only the cyclist does not need to run a dynamic calibration procedure when the power meter sensor is dismounted and mounted on another bike, but also accurate real-time monitoring and control of the cyclist power are made possible, to optimize the overall efficiency, as in [8], [9], [10], [11], [13]. Notice that the strategy presented in this paper has also been patented in [12].

The paper is organized as follows. Section II gives a complete description of the power meter device and its operating principles. In Section III, the angle estimation algorithm is described. In Section IV, the experimental results are presented concerning both the specific angle estimation and the corresponding power computation. Finally, Section V contains some conclusions and final remarks.

II. PROBLEM STATEMENT AND SENSOR DESCRIPTION

In this paper, the traction power estimation problem in bicycle is considered. In particular, the employed power meter device is a torque sensor mounted at the end of the left crank arm of the bicycle (see Figure 1). The device includes a custom pedal spindle equipped with two strain gauges, which measurement axes are orthogonal. The forces exerted on the pedal are indirectly obtained measuring the microscopic bending of the pedal spindle. The power meter is also equipped with a 6 d.o.f IMU, consisting of a triple-axis accelerometer and a 3 d.o.f gyrometer. The device can

The authors are with Dipartimento di Elettronica, Informazione e Bioingegneria, Politecnico di Milano, via G. Ponzio 34/5, 20133 Milano (Italy). E-mail to: dario.nava@polimi.it.

communicate using the ANT+ transmission protocol and the data recorded by the sensors can visualized in real-time on a suitable on-board computer mounted on the handlebars and downloaded to external devices.

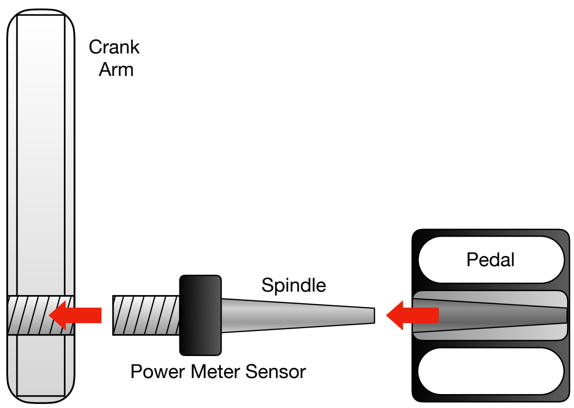

Fig. 1. Fastening scheme: the power meter is mounted at the end of the crank arm, the pedal fixed to the sensor spindle

The working priciple of the device is the following: during a ride, the total force F applied by the cyclist to the bycicle pedal can be seen as the resultant of two different and orthogonal components, as shown in Figure 2:

- a normal component F_N, applied along the crank arm longitudinal axis, always orthogonal to the pedal trajectory;
- a tangential conmponent F_T, which is orthogonal to the crank arm axis and always tangent to the pedal trajectory.

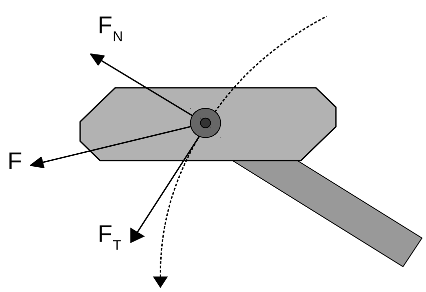

Fig. 2. Projection of the total force applied to the pedal along the two components: tangent F_T and normal F_N.

Since F_N is parallel to the crank arm axis, it is not involved into power generation. Thus, in order to estimate the power output of the cyclist, only the tangent component F_T has to be taken into account. The total power expended to make the bicycle move can be computed as:

$$P(t) = 2F_T(t) \cdot \omega(t) \cdot R, \tag{1}$$

where $\omega(t)$ and R are the rotational speed and the length of the crank arm respectively, and the multiplying factor 2

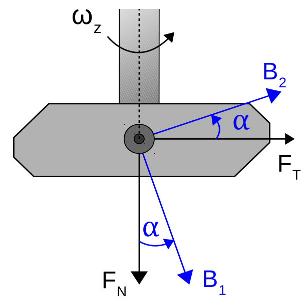

Fig. 3. Front view of the sensor, together with the force measurement reference frames.

takes into account the fact that the power generation can be assumed to be the same for both the bicycle pedals.

In Figure 3, the force reference frames are described. In an ideal setup, the two force measurement axes, B1 and B2, should be perfectly aligned with the directions of the normal force F_N and tangent force F_T, respectively. However, during standard use, since the device is manually fixed on the crank arm by the user, the force measurement frame $B1$-$B2$ is shifted by an assembly angle α with respect to the N-T frame (indicated in blue in Figure 3). As a consequence, the value of α has to be known in order to obtain the correct value of F_T from the measurement device.

In Figure 4 the IMU reference frames are described. The two reference axes x and y lie on the same plane defined by the force measurement frame, while the z axis completes the right-handed coordinate system. The three acceleration a_x, a_y and a_z are measured along the reference axes, while the angular velocities ω_x, ω_y and ω_z are measured by the gyros around x, y and z, respectively. As shown in the figure, β is defined as the angle between B1 and a_x. This angle is due to positioning errors during the fixing of the IMU while assembling the power meter device, and it is generally not negligible. However, since its value can be precisely computed as it will be shown in Section IV, it can be considered known.

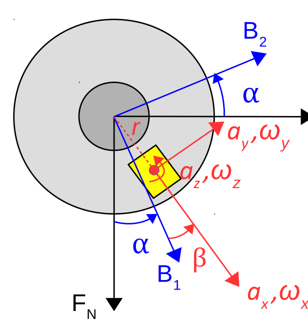

Fig. 4. Front view of the sensor with IMU reference frame.

Furthermore, the origin of the IMU reference frame is shifted with respect to the center force measurement frame of a distance r. The effects of this displacement are represented in Figure 5. By defining:

- C as the point in which the crank arm is fixed to the bicycle frame;
- O as the origin of the force axes (the center of the sensor spindle);
- O' as the origin of the acceleration axes;

it follows that $\overline{CO} \neq \overline{CO'}$. In particular, they are shifted by an angle δ, which can be obtained as

$$\delta = \tan^{-1}\left(\frac{r \cdot \sin(\alpha+\beta)}{R + r \cdot \cos(\alpha+\beta)}\right). \tag{2}$$

Hence, defining:

- a_N as the normal component of the acceleration, always orthogonal to the trajectory of the center O',
- a_T as the tangent component of the acceleration, always tangent to the trajectory of O',

the acceleration N-T frame is shifted with respect to the force N-T frame by the angle δ. Notice that the value of δ depends on the crank arm length R and the displacement r, that are known, and on the values of the two angles α and β, which instead have to be estimated.

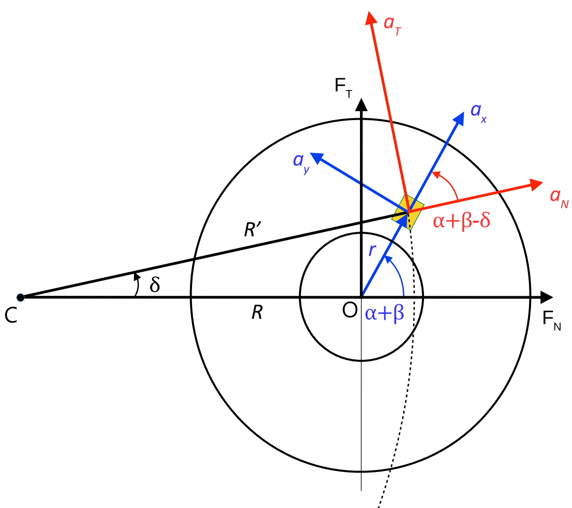

Fig. 5. Front view of the sensor.

It can be concluded that the problem of correctly estimating the power generated by the cyclist is then strictly connected to the estimation of the installing angle α of the power meter sensor with respect to the crank arm longitudinal axis. This problem will be analyzed in detail in the remainder of the paper. The estimation of β is instead less critical and will be briefly discussed in Section IV.

III. Adaptive Angle Estimation

In this section, the adaptive algorithm for the estimation of the angle α is described. The accurate knowledge of the value of such angle is of primary importance to correctly estimate the power output.

The proposed algorithm will be developed based on the acceleration measurements. The main reason behind this choice is the more regular shape of the acceleration signals with respect to the strain gauges signals, which allows to design a simple yet accurate estimation procedure. In order to derive the estimation algorithm, the following (mild) hypotheses are introduced:

- the angle β is independent from the value of α and is considered to be known. The output α_{est} of the estimation algorithm can be corrected according to the value of β at the end of the estimation procedure;
- the same reasoning can be extended to the angle δ. In general, its value depends on the value of α (Equation (2)), thus it has to be computed only at the end of the estimation procedure;
- the roll dynamics of the bicycle is neglected, as the bike is considered to proceed on a straight road with no significant curves or road banking (this could be avoided by suitably selecting the data for estimation);
- the origin of the force measurement frame is on the x axis of the acceleration measurements frame.

Under the above assumptions, the problem of estimating the α angle based on the inertial measurements reduces its dimensionality, turning from a 3D problem in the x-y-z frame into a 2D problem in the x-y plane. In fact, by imposing a null roll angle, we force the three signals a_z, ω_x and ω_y to be equal to zero. For this reason, the angle estimation algorithm relies exclusively on the three inertial measurements a_x, a_y and ω_z. Moreover, the only differences between the force measurement frame and the IMU frame are the origins of the reference systems, while the axes orientation are the same for both the frames. In order to switch from the measurement frames to the F_N-F_T frame, the same rotational matrix can be used (which is function of α). To obtain the normal and tangent forces from the measured signals F_{B_1} and F_{B_2}, it can be written that:

$$\begin{bmatrix} F_N \\ F_T \end{bmatrix} = \begin{bmatrix} \cos\alpha & -\sin\alpha \\ \sin\alpha & \cos\alpha \end{bmatrix} \begin{bmatrix} F_{B_1} \\ F_{B_2} \end{bmatrix}. \tag{3}$$

Similarly, defining the orthogonal and tangent accelerations as a_T and a_N, their values can be obtained from the acceleration measurements as follows:

$$\begin{bmatrix} a_N \\ a_T \end{bmatrix} = \begin{bmatrix} \cos\alpha & -\sin\alpha \\ \sin\alpha & \cos\alpha \end{bmatrix} \begin{bmatrix} a_x \\ a_y \end{bmatrix}. \tag{4}$$

The two accelerations a_T and a_N can be seen as the sum of different contributions depending on the gravity acceleration g and the angular velocity ω_z of the crank arm:

$$\begin{cases} a_T = g \cdot \cos(\omega_z t) + \dot{\omega}_z R \\ a_N = g \cdot \sin(\omega_z t) + \omega_z^2 R, \end{cases} \tag{5}$$

where R is the crank arm length. Supposing that the bicycle is proceeding at constant longitudinal speed $v = \tilde{v} > 0$ and the rear wheel is in traction, we can also assume the crank arm speed $\omega_z = \tilde{\omega}_z$ to be constant and, as a consequence, $\dot{\omega}_z = 0$. Hence, the Equation (5) becomes:

$$\begin{cases} a_T = g \cdot \cos(\tilde{\omega}_z t) \\ a_N = g \cdot \sin(\tilde{\omega}_z t) + \tilde{\omega}_z^2 R. \end{cases} \tag{6}$$

Let's consider now a time window which is multiple of the crank arm rotation period. Under this assumption, the mean value of the two gravitational terms $g \cdot \cos(\tilde{\omega}_z t)$ and $g \cdot \sin(\tilde{\omega}_z t)$ computed over the time window becomes equal to zero, since they are null mean signals. Thus, the mean values of the two accelerations a_T and a_N computed over the above mentioned time window ($\overline{a_T}$ and $\overline{a_N}$ respectively) can be obtained as:

$$\begin{cases} \overline{a_T} = 0 \\ \overline{a_N} = \tilde{\omega}_z^2 R > 0. \end{cases} \tag{7}$$

Following the above reasoning, the main idea behind the proposed algorithm arises, that is the fact that the true value of α is the one that, under the assumption of constant speed $\omega_z = \tilde{\omega}_z$ and sampling window multiple of $T = \frac{2\pi}{\omega_z}$, satisfies condition (7), when substituted in (4). The previous statement can be formalized as follows:

$$\alpha_{est} = \underset{\alpha}{\operatorname{argmin}} J(\alpha) \tag{8}$$

$$J(\alpha) = \Big(\frac{\overline{a_T}^2}{\overline{a_N}^2}\Big). \tag{9}$$

where α_{est} is the estimated mounting angle. Notice that minimizing $J(\alpha)$ corresponds to force the numerator term $\overline{a_T} \rightarrow 0$ and the denominator term $\overline{a_N} \rightarrow \tilde{\omega}_z^2 R$, thus matching the condition (7). Since in the cost function the mean values of the accelerations a_T and a_N are squared, there are two possible values of α which minimize $J(\alpha)$. In order to discriminate between the two, the hypothesis of positive forward speed is needed. If the bicycle is moving forward and the rear wheel is in traction, the cyclist is necessarily supplying a positive power to the mechanical system, which means that the force F_T has to be positive. Hence, the value of α is the one for which the mean value of F_T is positive over the time window in which the optimization is executed.

Finally, the value of the estimated angle α_{est} has to be corrected by taking into account the two angles β and δ. Since a positive β angle has the effect to increase the estimated value of α (see Figure 4), while a positive δ angle tends instead to reduce such value (as it can be see in Figure 5), the correct value of α is obtained as

$$\alpha = \alpha_{est} - \beta + \delta. \tag{10}$$

A. Data Selection Algorithm

While the assumption of finite number of rotation periods of the crank arm can be relaxed executing the estimation algorithm on large time windows, the hypothesis of constant positive crank arm speed ω_z is a necessary condition to obtain an accurate estimate of the sensor installation angle. Whereas during the average bicycle ride ω_z may span over a wide range of values, a constant speed detection algorithm is developed to identify the time windows in which the α estimation logic can be executed.

First of all, for null values of ω_z, it holds that $a_N = \tilde{\omega}_z^2 R = 0$ and the cost function (9) is not defined. Furthermore, for small values of ω_z, the mean values of the two accelerations a_T and a_N can be very similar, since the centrifugal terms becomes negligible. Thus, the minimization of the cost function may return a wrong value of α. In order to avoid these kind of problems, a threshold on the minimum value of ω_z is imposed.

Moreover, the sections of the measured signals in which high rotational accelerations of the crank arm are observed have to be discarded. To do so, two additional bounds are imposed on the rotational acceleration $\dot{\omega}_z(t)$, whose value can be easily obtained by differentiating the gyrometer signal $\omega_z(t)$. The first threshold is imposed directly on the maximum instantaneous value of $\dot{\omega}_z(t)$. The second one is instead imposed on the maximum average value of the rotational acceleration $\dot{\omega}_{z_{avg}}(t)$, computed over a certain constant time window T_ω:

$$\dot{\omega}_{z_{avg}}(t) = \int_{t-T_\omega}^{t} \dot{\omega}_z(t) \mathrm{d}t. \tag{11}$$

When one of the thresholds is exceeded, all the data from the sensors are discarded until the signals are back below the threshold. To avoid chattering, the signals need to remain under the thresholds for at least a time interval T_{hold} before the sensor signals is considered suitable for angle estimation.

The four inputs to the data selection algorithm are the crank arm rotational speed ω_z, its derivative $\dot{\omega}_z$ and the two acceleration signals a_x and a_y. The outputs of the logic are the constant speed detected sections ω_{z_c} and the two acceleration signals in correspondance of such sections a_{x_c} and a_{y_c}.

IV. Experimental Results

Experimental data have been recorded during a real bicycle ride, on which data selection and α estimation algorithms have been executed, as explained in Section III. The itinerary includes a series of non ideal conditions which can introduce errors in the estimate of α, such as road slope, road banking, curves and non-zero roll angle. This choice was made in order to test the robustness of the proposed approach.

During the experiment, the following signals are recorded with sampling time $T_s = 10ms$:

- the two forces F_{B_1} and F_{B_2}, with an accuracy of $10^{-3}Kg$;
- the two accelerations a_x and a_y, with an accuracy of $1mG$;
- the rotational speed ω_z, with an accuracy of $10^{-3}deg/s$.

and the following parameters of the bike and the power meter sensor are supposed to be given:

- displacement $r = 0.01m$,
- crank arm length $R = 0.175m$.

The true value of the angle α_{true} to be compared with α output of the angle estimation algorithm, and the value of the fixing angle β have been measured using a suitable static procedure structured as follows. First of all, the power meter sensor has to be mounted on the crank arm of the bicycle. Once the sensor is fixed to the bicycle frame, a sample mass m_s has to be hung to the spindle of the sensor. The action of such sample mass on the bicycle drive-train moves the crankarm-pedal assembly to his low configuration (crank arm perfectly orthogonal to the ground plane in the low position). In this static layout, it's clear that all the force exerted by the mass on the sensor spindle lies along the tangential direction in the *N-T* frame. Hence, since the strain gauges measure the two components F_{B_1} and F_{B_2} of such force, the angle α can be obtained from as:

$$\alpha_{true} = \tan^{-1}\left(-\frac{F_{B_2}}{F_{B_1}}\right). \tag{12}$$

Moving to the accelerometers frame, during the static procedure the only acceleration measured by the inertial sensor is the gravitational one, which points (by definition) in the same direction of the sample mass weight force. Since the two accelerometer axes are shifted of an angle β with respect to the force measurement frame, combining force and acceleration measures, it follows that:

$$\alpha_{true} + \beta = \tan^{-1}\left(-\frac{a_y}{a_x}\right), \tag{13}$$

thus β can be obtained as:

$$\beta = \tan^{-1}\left(-\frac{a_y}{a_x}\right) - \tan^{-1}\left(-\frac{F_{B_2}}{F_{B_1}}\right). \tag{14}$$

At the end of the procedure, by substituting the values of F_{B_1}, F_{B_2}, a_x and a_y in Equations (12) and (14), the two angles $\alpha_{true} = 65.19°$ and $\beta = 0.24°$ are obtained.

A. Data selection and α estimation

As a first step, the data has been divided in eight time windows with a fixed duration of 300s and all the signals have been low-pass filtered at $2Hz$. Hence, the data selection procedure described in Section III-A has been performed on each data set. The parameters set for the algorithm are the following:

- $\omega_{z_{min}} = 6rad/s$, as a threshold on the rotational speed;
- $|\dot{\omega}_z|_{max} = 2.5rad/s^2$, as a threshold on the instantaneous rotational acceleration;
- $|\dot{\omega}_{z_{avg}}|_{max} = 0.06rad/s^2$, as a threshold on the average rotational acceleration;
- $T_{hold} = 5s$, as the minimum data discarding time.

An example of the data selection procedure can be seen in Figure 6. In the first subfigure on the top, the light blue signal represents the original signal ω_z of the gyro, while the constant speed sections selected from the algorithm (ω_{z_c} signal) are represented in red. In the selected sections, ω_{z_c} coincides with ω_z, while it is set to zero if the data has to be discarded. From the figure, it can be noticed that the algorithm is actually capable to recognize the constant speed sections. Moreover, by looking at the acceleration signals, it is easy to understand why two different thresholds are necessary. The threshold on the instantaneous acceleration $\dot{\omega}_z(t)$ guarantees a fast response to speed changes. On the other hand, $\dot{\omega}_z$ is obtained by differentiating the gyro signal and thus its noise-signal ratio is very high. As a consequence, the value of the threshold has to be taken large enough to avoid chattering effects caused by the noise, by making the constant speed condition less restrictive. This problem can be successfully counteracted by introducing the second threshold on $\dot{\omega}_{z_{avg}}(t)$, which is less noisy than $\dot{\omega}_z(t)$, but with the disadvantage of having a slower response to speed variations.

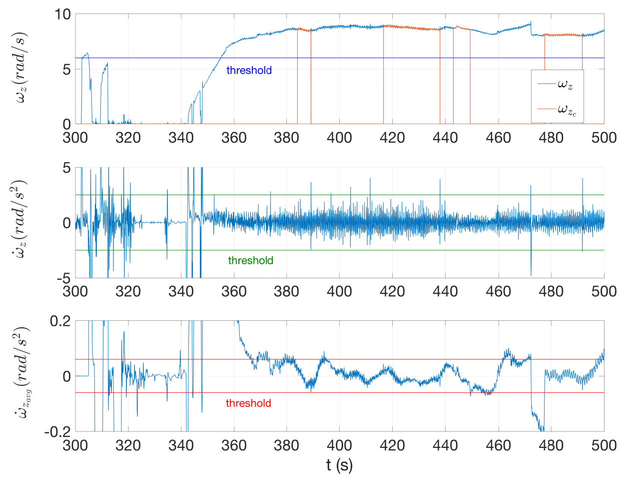

Fig. 6. Data selection on the road test dataset.

Once the useful sections of the dataset have been identified, the two outputs of the data selection algorithm a_{x_c} and a_{y_c} are substituted in (9) to obtain the estimated angle α_{est}. The procedure is repeated for all the 8 time windows in which the dataset is divided. The results are summarized in Table I.

Time Window $n°$	Estimated Angle α_{est} [deg]
1	62.65
2	62.60
3	62.62
4	62.84
5	62.56
6	62.44
7	62.76
8	62.49
Average	62.62 ± 0.22

TABLE I

ANGLE ESTIMATION ALGORITHM: NUMERICAL RESULTS.

The average value of the estimated angle α_{est} has been corrected taking into account the two angles β and δ. The value of β has already been estimated in Section IV. An approximation of the angle δ instead has been computed substituting α_{est} and β in the equation (2). Finally, the value of α has been obtained substituting the values of α_{est}, β and δ_{est} in the (10). All the results are summarized in Table II.

At the end of the procedure, the value of α is estimated with an average error $\varepsilon_{avg} = 0.10°$, while the maximum error is $\varepsilon_{max} = 0.32°$. This result confirms the effectiveness of the proposed technique. In the next subsection, the results will be assessed in terms of estimate output power.

	[deg]
α_{est}	62.62 ± 0.22
β	0.24
δ_{est}	2.91
α	65.29 ± 0.22
α_{true}	65.19

TABLE II
FINAL RESULTS

B. Effect on energy estimation

In order to asses the effects of an error on the α estimate on the power output computation, a sensitivity analysis has been carried out on the energy consumed by the cyclist during a certain period of time. Looking at the total energy, some information about the general trend (mean value) of the power error can be obtained. Once α is known, the tangential force F_T can be obtained from the raw force measurement by means of (3). Thus, the power output transmitted by the cyclist to the rear wheel of the bicycle can be obtained by substituting the value of F_T in the equation (1).

Starting from the power $P(t)$, the total energy consumed over a certain time window $[t-\bar{t}, t]$ can be computed as:

$$E(\alpha) = \int_{t-\bar{t}}^{t} P(t, \alpha) \mathrm{d}t. \tag{15}$$

To assess the robustness of the proposed algorithm, the energy is computed also for different values of α, obtained as a variation from α_{true}. The energy error can be computed as:

$$E_{error} = \frac{E(\alpha) - E(\alpha_{true})}{E(\alpha_{true})}. \tag{16}$$

The results of the analysis are represented in Figure 7. The trend of the energy error is essentially linear with respect to the value of the α error, since every degree of error on the value of α becomes approximately a 2% error on the computed total energy. Thus, being $0.32°$ the maximum α error obtained with the proposed estimation procedure, it can be concluded that the mean error on the power output is approximately 0.65%. This results confirm the effectiveness of the approach proposed in this paper also in the estimation of the power transmitted to the rear wheel within a bicycle ride.

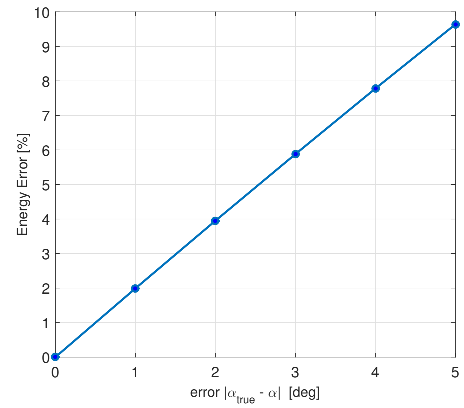

Fig. 7. Energy error corresponding to different α errors.

V. CONCLUSIONS

In this work, the problem of estimating the cyclist power using a power meter sensor mounted between the crank arm and the pedal has been considered. An approach based on the accelerations measurements has been proposed to correctly estimate the installation angle α of the power meter sensor. Results have shown that the estimation procedure is accurate enough for power monitoring and control. In fact, the error on the energy computation turns out to be less than 1% of the reference value. Future work will be dedicated to the application of such a sensing strategy to power monitoring and control and efficiency optimization.

REFERENCES

[1] E. F. Coyle, M. E. Feltner, S. A. Kautz, et al., *Physiological and biomechanical factors associated with elite endurance cycling performance*, Medicine and Science in Sports and Exercise, vol. 23, No. 1, 1991.

[2] S. K. Gharghan, R. Nordin, M. Ismail, *Empirical investigation of pedal power calculation techniques for track cycling performance measurement*, IEEE Student Conference on Research and Development (SCOReD), 16-17 December 2013, Putrajaya, Malaysia.

[3] S. A. Sparks, B. Dove, C. A. Bridge, A. W. Midgley, and L. R. McNaughton, *Validity and Reliability of the Look Keo Power Pedal System for Measuring Power Output During Incremental and Repeated Sprint Cycling*, International Journal of Sports Physiology and Performance, 10, 39-45, 2015.

[4] A. S. Gardner , S. Stephens, D. T. Martin, E. Lawton , H. Lee , and D. Jenkins, *Accuracy of SRM and Power Tap Power Monitoring Systems for Bicycling*, Medicine and Science in Sports and Exercise, vol. 36, No. 7, 2004.

[5] C. R. Abbiss, M. J. Quod, G. Levin, D. T. Martin, P. B. Laursen, *Accuracy of the Velotron Ergometer and SRM Power Meter*, International Journal of Sports Medicine, 30(2): 107-112, 2009.

[6] A. V. Pigatto, K. O. A. Moura, G. W. Favieiro and A. Balbinot, *A new Crank Arm Based Load Cell, with built-in conditioning circuit and strain gages, to measure the components of the force applied by a cyclist*, 38th Annual International Conference of the IEEE Engineering in Medicine and Biology Society (EMBC), 2016.

[7] R. J. Wyatt, D. J. Seguin, R. B. Knapp, *Systems and methods of power output measurement*, US Patent No. US 8,122,773B2, February, 28, 2012.

[8] K. J Astrom, R. E Klein, and A. Lennartsson. Bicycle dynamics and control: adapted bicycles for education and research. *IEEE Control Systems*, 25(4):26–47, 2005.

[9] M. Corno, P. Giani, M. Tanelli, and S. M. Savaresi. Human-in-the-loop bicycle control via active heart rate regulation. *IEEE Transactions on Control Systems Technology*, 23(3):1029–1040, 2015.

[10] M. Corno, F. Roselli, and S. M. Savaresi. Bilateral control of Senza: series hybrid electric bicycle. *IEEE Transactions on Control Systems Technology*, 25(3):864–874, 2017.

[11] J. Guanetti, S. Formentin, M. Corno, and S. M. Savaresi. Optimal energy management in series hybrid electric bicycles. *Automatica*, 81:96–106, 2017.

[12] S.M. Savaresi, G. Favero, S. FORMENTIN, D. Nava
Dispositivo e metodo per la determinazione della potenza impressa sui pedali di una bicicletta.
Applicant: Favero Electronics S.r.l. and Politecnico di Milano
Patent number (Italian Patent): 102017000043114. April 20, 2017.

[13] N. Rosero, J. Martinez, and H. Leon. A bio-energetic model of cyclist for enhancing pedelec systems. In *20th World Congress of the International Federation of Automatic Control (IFAC 2017)*, 2017.